Payload Length and Rate Adaptation for Multimedia Communications in Wireless LANs

Sayantan Choudhury, *Student Member, IEEE,* and Jerry D. Gibson, *Fellow, IEEE*

***Abstract*— We provide a theoretical framework for cross-layer design in multimedia communications to optimize single-user throughput by selecting the transmitted bit rate and payload size as a function of channel conditions for both additive white Gaussian noise (AWGN) and Nakagami-m fading channels. Numerical results reveal that careful *payload length* adaptation significantly improves the throughput performance at low signal to noise ratios (SNRs), while at higher SNRs, *rate* adaptation with higher payload lengths provides better throughput performance. Since we are interested in multimedia applications, we do not allow retransmissions in order to minimize latency and to reduce congestion on the wireless link and we assume that packet loss concealment will be used to compensate for lost packets. We also investigate the throughput and packet error rate performance over multipath frequency selective fading channels for typical payload sizes used in voice and video applications. We explore the difference in link adaptation thresholds for these payload sizes using the Nafteli Chayat multipath fading channel model, and we present a link adaptation scheme to maximize the throughput subject to a packet error rate constraint.**

***Index Terms*— Multimedia communications, payload adaptation, rate adaptation, frequency selective fading, performance evaluation**

I. Introduction

Wireless local area networks (WLANs) are rapidly becoming part of our network infrastructure. The IEEE 802.11 WLAN physical layer (PHY) supports multiple data rates by using different modulation and channel coding schemes. For instance, the IEEE 802.11a networks have 8 different modes with varying data rates from 6 to 54 Mbps [1]. However, due to the packet headers from higher layers, as well as the various overheads in the medium access control (MAC) scheme, there is a significant reduction in effective throughput, where effective throughput (or goodput) is defined as the ratio of the expected delivered data payload to the expected transmission time [2]. Moreover, most voice and video applications tend to use very small payload sizes to ensure reliable, low delay delivery. This results in a further significant loss in effective throughput. A cross-layer based design approach is presented in this paper whereby a joint adaptation of the PHY and MAC layer parameters show a significant performance improvement.

Manuscript received May 4, 2006; revised November 15, 2006. This research has been supported by the California Micro Program, Applied Signal Technology, Dolby Labs, Inc., Mindspeed, and Qualcomm, Inc., by NSF Grant Nos. CCF-0429884 and CNS-0435527, and by the UC Discovery Grant Program and Nokia, Inc. A portion of these results appeared in the IEEE 63rd Vehicular Technology Conference, Melbourne, Australia, May 2006 and in the IEEE Wireless Communications and Networking Conference, Las Vegas, NV, April 2006.

The authors are with the Department of Electrical Engineering, University of California, Santa Barbara, CA 93106 USA (email:sayantan@ece.ucsb.edu; gibson@ece.ucsb.edu).

The effective throughput is affected by a number of parameters, including transmission rate, payload and header size, constellation size, transmitted power, and received noise characteristics. When the channel is time varying in nature, the transmission parameters should be adapted according to channel conditions to improve link performance. The mechanism to select one of the multiple available transmission rates is referred to as *link adaptation*. The current link adaptation schemes used in IEEE 802.11a wireless cards are proprietary (mostly based on received signal strength and packet error rates) and in many cases can lead to inefficient bandwidth utilization and unnecessary rate adaptation. In this paper, we analyze the improvement in single-user effective throughput provided by link adaptation by varying the data rate and packet length as a function of channel conditions. For theoretical analyses, we consider both AWGN and block fading Nakagami-m channels.

The joint PHY-MAC based cross-layer design approach described above is then extended to multipath fading channels. A critical component of any link adaptation scheme is the identification of signal to noise ratio (SNR) thresholds at which to alter the link adaptation parameters [3]. We conduct exhaustive simulations to identify the SNR thresholds for 3 different payload sizes of 20 bytes, 200 bytes and 2000 bytes, respectively. These payload sizes cover a wide range of applications from various voice codecs to H.264 video-conferencing applications along with various data applications like web browsing, ftp, etc. For example, in Table I we show the I-frame and average P-frame sizes for different video sequences with different quantization parameters (QPs) coded using H.264 reference software JM10.1 with GOPS = 90 frames, frame rate = 15 frames per second (fps), 5 reference frames, and no packet loss [4]. As can be seen from Table I, the average size of P frames for silent.cif varies from 725 to 1272 bytes as the QP is decreased from 30 to 26 and the average size of P frames for paris.cif varies from 1683 to 2924 bytes as the QP is reduced from 30 to 26. As we show in this paper, using a higher payload size (around 2000 bytes) for video transmission can significantly improve the throughput performance in good channel conditions. However, in environments where the packet error rate is high (low SNR regions), a lower payload size (200 bytes) might be preferable. Furthermore, a 200 bytes payload size corresponds to 25 ms of G.711 speech coded at 64 Kbps while a 20 byte payload would correspond to 20 ms of G.729 speech coded at 8 Kbps.

Payload adaptation is a critical component in improving the multimedia performance over IEEE 802.11 networks. Some preliminary investigations on the voice capacity of an

TABLE I: H.264 codec performance of three different video sequences

Video	silent.cif 		paris.cif 		stefan.cif 	
Typical application	video conference		news broadcast		sports broadcast	
QP	26	30	26	30	26	30
Avg psnr(dB)	36.69	34.22	36.59	33.45	36.69	33.47
Bit rate (kbps)	169.5	97.8	373.5	218.9	1396.8	404.6
I frame size (bytes)	13945	8826	19886	14390	30432	15978
Average of P frame size (bytes)	1272	725	2924	1683	11429	3230
Variance of P frame size (bytes)	412	254	322	219	1544	625

IEEE 802.11 b network was conducted in [5] where it was observed that in good channel conditions, a higher number of voice users can be supported by using larger payload sizes. An early investigation of the effect of payload size on throughput was conducted in [6]. We extend their work by taking into account various packet header and protocol overheads in the context of IEEE 802.11a wireless LANs, which have a tremendous impact on the effective throughput. Rate adaptation using a theoretical framework to evaluate the throughput has been investigated in [2]. A computationally expensive dynamic programming approach was proposed by the authors to find the optimal data rates that can be used for fairly simple wireless channel variation models with known probability of transitions from *good* to *bad* states and vice-versa, using a discrete-time Markov chain. The effect of multipath fading was not considered there. As we show in this paper, consideration of multipath fading can result in significantly different SNR thresholds for switching between data rates in IEEE 802.11a WLANs. A link adaptation strategy for IEEE 802.11b was provided in [7]. Frame lengths were classified into 3 broad classes: 0-100 bytes, 100-1000 bytes and 1000-2400 bytes. In this paper, we consider payload length as an optimization parameter and propose a cross-layer scheme that jointly optimizes payload length and data rate for a given channel condition. Our novel algorithm takes into account the tight coupling between payload length and data rate to maximize the single-user throughput based on the channel conditions. The theoretical formulation allows payload length to be varied continuously over a wide range and we provide a mathematical framework to dynamically adapt the payload length to maximize the throughput for AWGN and different fading channels. Our results indicate that both the payload length as well as the data rate is dependent on the channel under consideration. The algorithm does not require any changes in the current MAC operations and the data rates and payload lengths can be varied with the received SNR. The optimal payload length obtained by our algorithm can also be used over rate adaptation only algorithms such as AutoRate Fallback (ARF) protocol [8] and Receiver-Based Auto-Rate (RBAR) [9] protocol.

Link adaptation for Hiperlan/2 networks is considered in [10], [11]. In [12], the impact of frequency selectivity on link adaptation algorithms was considered. However, in Hiperlan/2 the payload size does not impact the link adaptation algorithm, which is quite different from the IEEE 802.11 MAC where payload size has a tremendous effect on the throughput [13]. In this paper, we investigate the effect of frequency selectivity and payload length variation on single-user throughput. The payload sizes we consider represent a wide range of data, voice and video applications. We also show the limitations of link adaptation schemes that just consider the path-loss and shadowing effects of the wireless channel and neglect the multipath fading effects.

A major contribution of this paper is to provide realistic estimates of throughput and packet error rates for various payload sizes that can be used for cross layer design for multimedia communications. Analytical calculation of packet error rate in multipath fading taking into account the impact of forward error correction and interleaving is quite difficult and hence we conduct exhaustive Monte Carlo simulations to accurately estimate the packet error rates. The throughput and packet error rate curves along with the link adaptation tables can be used for cross-layer design to identify the SNR operating regions and corresponding data rates to optimize multimedia applications. To our knowledge, this is the only joint PHY/MAC based cross-layer design scheme where the payload length and data rate are jointly optimized to maximize throughput. Moreover, there is no prior documentation of SNR thresholds, throughput and packet error rate curves in multipath fading for different payload sizes used in voice and video communications over IEEE 802.11a WLANs.

The paper is outlined as follows. In the next section, we review the protocol overheads in IEEE 802.11a. In Section III we provide a brief description of the theoretical model to evaluate single-user throughput in 802.11a systems and use it to plot the payload lengths versus transmission rate under different channel conditions. Section IV contains numerical results for our rate and payload length adaptation scheme, and provides the transmission rate/packet length combinations that maximize effective throughput as a function of average symbol SNR for AWGN and Nakagami-m fading channels. In Section V, we investigate the effect of multipath fading on link adaptation thresholds for the different payload lengths using the Nafteli Chayat channel model. Section VI states conclusions and future research directions.

II. Protocol overheads in IEEE 802.11a

In this section, we investigate the effect of payload length variation on the single-user throughput for a wireless link. We first provide a brief overview of the various packet headers and the protocol overheads [2], [14].

The IEEE 802.11 MAC specifies two different mechanisms, namely the contention-based Distributed Coordination Function (DCF) and the polling-based Point Coordination Function (PCF), with the DCF being more widely used. The DCF uses carrier sense multiple access with collision avoidance (CSMA/CA) for medium access. DCF has two mechanisms for packet transmission, the default basic access mechanism and the optional request-to-send/clear-to-send

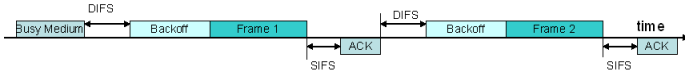

Fig. 1: Successful transmission using DCF

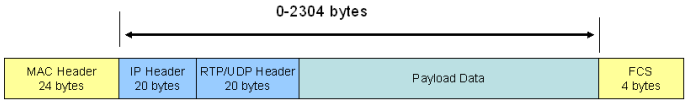

Fig. 2: Frame format of a data frame MPDU

mechanism (RTS/CTS). The basic access mechanism is a two-way handshaking technique where the destination transmits a positive acknowledgment (ACK) on successful packet reception. In the event of packet loss either by bit errors or collisions, a random backoff is initiated in order to reduce the probability of collisions. An explicit ACK transmission is required since these wireless transceivers are generally half-duplex, i.e. they do not transmit and receive at the same time and hence cannot detect a collision by listening to its own transmission. We consider the DCF with basic access in this paper.

A. IEEE 802.11 Distributed Coordination Function

The DCF [15] uses CSMA/CA for medium access among multiple stations. A station senses if the medium has been idle for a period of time equal to the Distributed Interframe Space (DIFS) before transmitting a packet. On the other hand, if the channel is sensed busy during the DIFS interval, then it monitors the channel until it is idle for a DIFS interval and then waits for a random period, referred to as the *backoff window* or *contention window*, before transmitting a packet. This is called the *access deferral* and helps in reducing the probability of collisions among multiple stations.

In wireless networks, the destination needs to send a positive ACK on successful reception of a packet. The period of time between packet and ACK transmission is called the Short Interframe Space (SIFS). The SIFS time plus the propagation delay is less than the DIFS interval so that other stations cannot determine the channel to be idle for a DIFS interval before the end of the ACK transmission. The timing diagram of a successful transmission is shown in Fig. 1.

B. MAC/PHY overheads

The OFDM physical layer convergence procedure (PLCP) is used for controlling frame exchanges between the MAC and PHY layers. The frame format for the MAC data frame is given in Fig. 2. Each MAC frame or MAC protocol data unit (MPDU) consists of MAC header, variable length frame body and a frame check sequence (FCS). The MAC header and FCS consist of 28 bytes and the ACK is 14 bytes long. The frame body varies from 0-2304 bytes including the RTP/UDP and IP headers. The RTP and UDP overhead for multimedia traffic is 12 and 8 bytes, respectively, and another 20 bytes is added for the IP header.

The IEEE 802.11a wireless systems operate in the 5 GHz Unlicensed National Information Infrastructure (U-NII) band, and use twelve 20 MHz channels from the U-NII lower band (5.15-5.25 GHz), U-NII mid-band (5.25-5.35 GHz) and U-NII upper band (5.725-5.825 GHz) with the first 8 channels dedicated for indoor use. Each 20 MHz channel is composed of 52 subcarriers, with 48 being used for data transmission and the remaining 4 used as pilot carriers for channel estimation and phase tracking needed for coherent demodulation. The 802.11a PHY provides 8 modes with varying data rates from 6 to 54 Mbps by using different modulation and coding schemes as shown in Table II. Forward error correction (FEC) is done by using rate 1/2 convolutional coding and bit interleaving for the mandatory rates and using puncturing for the higher rates. A detailed description of OFDM systems and their applications to wireless LANs can be found in [16], [17].

TABLE II: PHY Modes in IEEE 802.11a

Mode	Modulation	Code Rate	Data Rate	Bytes per Symbol
1	BPSK	1/2	6 Mbps	3
2	BPSK	3/4	9 Mbps	4.5
3	QPSK	1/2	12 Mbps	6
4	QPSK	3/4	18 Mbps	9
5	16-QAM	1/2	24 Mbps	12
6	16-QAM	3/4	36 Mbps	18
7	64-QAM	2/3	48 Mbps	24
8	64-QAM	3/4	54 Mbps	27

A PLCP Protocol Data Unit (PPDU) is formed by adding a PLCP preamble and header to the MPDU. The PLCP header (excluding the service field) is transmitted using BPSK modulation and rate 1/2 convolutional coding. The six "zero" tail bits are used to unwind the convolutional code, i.e. to reset it to the all zero state, and another 16 bits is used by the SERVICE field of the PLCP header. A few important parameters of the IEEE 802.11a OFDM PHY are summarized in Table III.

TABLE III: IEEE 802.11a OFDM PHY characteristics

Parameter	Value	Notes
tSlot	$9\mu s$	Slot Time
tSIFS	$16\mu s$	SIFS Time
tDIFS	$34\mu s$	DIFS = SIFS + 2 * Slot
CW_{min}	15	min. contention window size
CW_{max}	1023	max. contention window size
tPLCP_Preamble	$16\mu s$	PLCP preamble duration
tPLCP_SIG	$4\mu s$	PLCP SIGNAL Field duration
tSymbol	$4\mu s$	OFDM symbol interval

III. Throughput Analysis in IEEE 802.11a wireless networks

In this section we present a mathematical framework for single user throughput optimization by varying the payload length. We provide an integrated framework for link adaptation by considering various physical and MAC layer adaptation

parameters. In particular, we have developed an adaptive frame length transmission algorithm using adaptive modulation as supported by IEEE 802.11a and adaptive framing in the MAC layer.

We define *throughput* as the number of payload bits per second received correctly. For the initial analysis, we consider the effects of payload variation in additive white Gaussian noise (AWGN) channels and assume that the acknowledgments from the receiver are error-free. Throughput corresponding to PHY mode j is given by:

$$T(j) = \frac{L}{L + C_j} * R_j * P_s^j(\gamma_s, L) \tag{1}$$

where
L: payload length in bits,
C_j: header and DCF overhead corresponding to rate 'j' in bits,
R_j: data rate corresponding to PHY mode j,
$P_s^j()$: packet success rate (PSR) defined as the probability of receiving a packet correctly corresponding to PHY mode j
γ_s: SNR per symbol.

C_j takes into account the CSMA/CA channel access time and the header overheads as specified by the IEEE 802.11 protocol. The time delay is converted to bytes for the purpose of optimization by the following expression :

$$C_j = R_j * T_{ho} \tag{2}$$

where R_j is transmission rate corresponding to PHY mode 'j' and T_{ho} is the total protocol overhead and can be evaluated as in [2].

We assume hard-decision Viterbi decoding at the receiver. For a L bits long packet, the probability of packet error can be bound by [18]:

$$P_e^j(L, \gamma_s) \leq 1 - (1 - P_u^j(\gamma_s))^L \tag{3}$$

where $P_u^j(\gamma)$ is the union bound of the first-event error probability corresponding to PHY mode j [19] and is given by:

$$P_u^j(\gamma_s) = \sum_{d=d_{free}}^{\infty} a_d \cdot P_d(\gamma_s) \tag{4}$$

with d_{free} being the free distance of the convolutional code selected in PHY mode j and a_d is the total number of error events of weight d, that can be obtained from [19]. For hard-decision decoding with probability of bit error ρ, $P_d(\gamma_s)$ is given by [20]

$$P_d(\gamma_s) = \begin{cases} \sum_{k=(d+1)/2}^{d} \binom{d}{k} \cdot \rho^k \cdot (1-\rho)^{d-k} & \text{if d is odd} \\ \frac{1}{2} \cdot \binom{d}{d/2} \cdot \rho^{d/2} \cdot (1-\rho)^{d/2} & \\ + \sum_{k=d/2+1}^{d} \binom{d}{k} \cdot \rho^k \cdot (1-\rho)^{d-k} & \text{if d is even} \end{cases} \tag{5}$$

The bit error probability ρ computation for AWGN for the various PHY modes in IEEE 802.11a is described in [2]. In order to compute the packet error rate in fading environments, we employ average bit error probability expressions for BPSK, and M-ary QAM in Nakagami-m fading [21]. The Nakagami-m fading model is used to describe a wide range of fading models and includes the Rayleigh distribution (m = 1) as a special case. The fade is assumed constant for the entire packet duration over all subcarriers. The average bit error for BPSK over a Nakagami fading channel for integer m and average SNR per symbol γ_s is given by [21]:

$$\rho = \frac{1}{2}\left[1 - \mu \sum_{k=0}^{m-1} \binom{2k}{k} \left(\frac{1-\mu^2}{4}\right)^k\right] \tag{6}$$

where,

$$\mu = \sqrt{\frac{\bar{\gamma}_s}{m + \bar{\gamma}_s}}$$

The bit error probability for M-ary QAM in Nakagami-m fading can be derived from [21] as:

$$\rho \cong 4\left(\frac{\sqrt{M}-1}{\sqrt{M}}\right)\left(\frac{1}{\log_2 M}\right) \sum_{i=1}^{\sqrt{M}/2} \frac{1}{2}\left[1 - \mu \sum_{k=0}^{m-1} \binom{2k}{k} \left(\frac{1-\mu^2}{4}\right)^k\right] \tag{7}$$

where

$$\mu = \sqrt{\frac{1.5(2i-1)^2 \bar{\gamma}_s}{m(M-1) + 1.5(2i-1)^2 \bar{\gamma}_s}}$$

The packet success rate (PSR) is given as :

$$P_s^j(\gamma_s, L) = 1 - P_e^j(L, \gamma_s) \tag{8}$$

where L is the packet length including the various overheads in bits.

In order to find the optimal payload length L^*, we assume the payload length L varies continuously. Differentiating Eq. (1) with respect to L and setting it to zero with packet success rate given by Eq. (8), the optimal payload length at a given SNR is:

$$L^* = -\frac{C_j}{2} + \frac{1}{2}\sqrt{C_j^2 - \frac{4 * C_j}{\log(1 - P_u^j(\gamma_s))}} \tag{9}$$

Some key assumptions in our model are single transmission, no losses due to collisions, i.e. packet losses are caused only by bit errors in AWGN and fading environments, and the transmission of acknowledgments is error free. The mobile terminals require an accurate estimation of the SNR at the access points. A scheme assuming a linear mapping between received signal strength (RSS) and SNR is proposed in [7]. Thus based on the RSS of the ACK frames from the access points, the mobile station can estimate the SNR at the receiver.

IV. Numerical Results

A. Impact of payload length on effective throughput

The variation of throughput with payload lengths at an SNR of 2 dB and 5 dB in an AWGN channel is shown in Figs. 3 and 4, respectively. The higher rates supported in IEEE 802.11a are not visible in the plots due to the high packet error rates at low SNRs that reduces the effective throughput at these rates to zero. For example, in Fig. 3, at an SNR of 2 dB, only the curve for PHY mode 1 corresponding to 6 Mbps is evident, since the higher transmitted data rates have packet error rates that reduce the effective throughput to near zero. We varied the payload lengths from 1-2264 bytes and added 40 bytes of RTP/UDP/IP

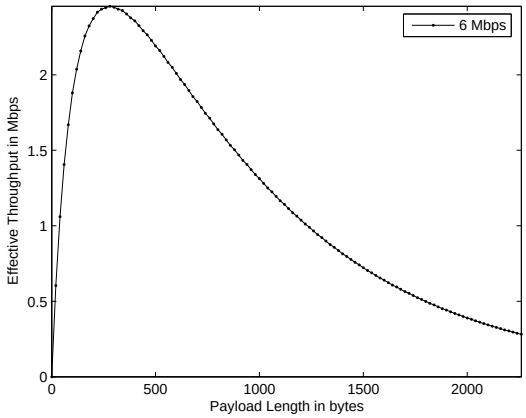

Fig. 3: Throughput versus payload length at an SNR of 2 dB in AWGN channel

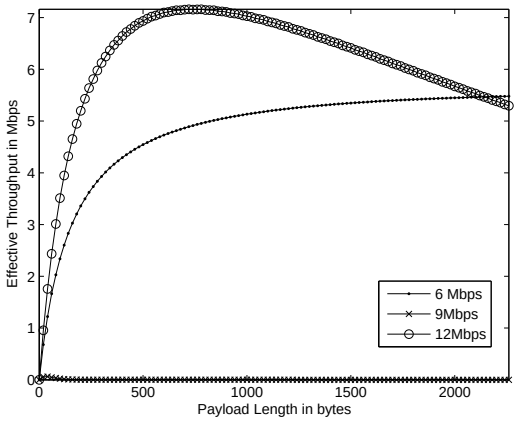

Fig. 5: Throughput versus payload length at an average SNR of 12 dB in Rayleigh fading channel

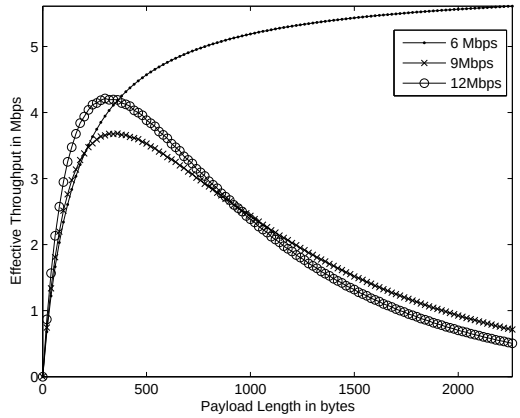

Fig. 4: Throughput versus payload length at an SNR of 5 dB in AWGN channel

header used for multimedia traffic. The maximum allowable MPDU frame body length is 2304 bytes without fragmentation [15]. The plots show that there is an optimal payload length and rate corresponding to the received SNR for throughput maximization. This is quite intuitive since at a given SNR, increasing the data rate, i.e. bits per constellation or payload length, would initially cause an increase in throughput but it reaches an optimum value beyond which higher packet error rate (Eq. (3)) leads to a decrease in throughput. As shown in Fig. 3, at an SNR of 2 dB, only PHY mode 1 corresponding to 6 Mbps is used, and the optimal payload length is around 280 bytes corresponding to an effective throughput of 2.45 Mbps. Thus, there is a significant reduction in the effective throughput from the supported data rate of 6 Mbps and reducing the payload length or increasing it does not increase throughput at such low SNRs. For instance, the effective throughput achieved at an SNR of 2 dB in AWGN with a 20 byte payload is 0.6 Mbps and with a 2000 byte payload, it is around 0.4 Mbps.

A similar observation is made from Fig. 4 where the optimal payload length for 12 Mbps data rate is around 400 bytes corresponding to a throughput of 4.2 Mbps. However, by employing a lower constellation size using BPSK with rate 1/2 convolutional coding (6 Mbps data rate), we observe that we can use much higher payload lengths (greater than 2000 bytes) to achieve a higher throughput (5.5 Mbps). Hence, corresponding to every SNR, there is an optimal data rate and payload length that maximizes the effective throughput. The effective throughput obtained using the theoretical model is very close to that obtained by simulations. In [22], it was observed there is a 0.5 dB difference in the channel SNR between the theoretical results and those obtained by simulation. The impact of retransmissions is not considered here since retransmissions increase the latency significantly that can be unacceptable for multimedia applications. Hence, we rely on packet loss concealment to conceal lost packets.

We also observe a similar behavior for fading channels. In particular, we plot the throughput curves for an average SNR of 12 dB for a Nakagami-m fading channel with m set equal to one (which corresponds to Rayleigh fading) in Fig. 5. As seen from Fig. 5, the optimal payload length is around 740 bytes with an effective throughput of 7.2 Mbps. A 2000 byte payload length would correspond to a throughput of 5.7 Mbps and a 20 byte payload length would decrease the effective throughput to 0.9 Mbps. It is interesting to observe from this plot that PHY mode 2 corresponding to 9 Mbps would not be used since the packet error rate at this mode for an average SNR of 12 dB in Rayleigh fading, is intolerable. Instead PHY mode 3 corresponding to 12 Mbps, which has a larger constellation size (QPSK as compared to BPSK in PHY mode 2), has a significantly lower bit error rate and hence lower packet error rate. This behavior for PHY mode 2 has been widely described in the literature and is attributed to the poor performance of the rate 3/4 punctured convolutional codes for PHY mode 2 compared to a rate 1/2 convolutional code for PHY mode 3 [2]. This results in the effective throughput for PHY mode 3 being significantly higher compared to PHY mode 2.

Selecting the proper data rate along with payload size is crucial for maximizing spectral efficiency. Selecting the lowest rate always, which uses BPSK, is too conservative an approach, while selecting a much higher data rate can cause a

severe degradation in overall throughput. Another interesting observation from the above plots, is that there are relatively sharp peaks in the throughput plots for lower SNRs, while a more gradual transition is observed for higher SNRs, i.e for the 2 dB case, there is a small range of payload lengths around 280 bytes that can be selected for optimal performance, whereas for the 12 dB case, there is a much broader range of payload lengths around 740 bytes. This suggests that the payload length adaptation is more crucial at lower SNRs. We discuss this in greater detail in the following section.

B. Optimal Payload Length and Rate adaptation

In this section, we present the optimal payload length and rate adaptation for AWGN and Rayleigh fading channels. In Fig. 6(a), we plot the effective throughput as a function of SNR obtained by a joint adaptation of payload lengths and data rate based on our theoretical framework for an AWGN channel. The resulting transmitted data rates are shown in Fig. 6(b) and the corresponding payload lengths are shown in Fig. 6(c).

The optimal payload length and rate adaptation for a slowly fading Rayleigh channel are shown in Fig. 7. The effective throughput is plotted against average symbol SNR in Fig. 7(a), while Figs. 7(b) and 7(c) indicate the optimal data rate and payload size. It is observed from Figs. 6(c) and 7(c) that payload variation is more significant at the lower SNR regions while at higher SNRs, a larger payload length can be used with careful data rate adaptation. Moreover, the range of SNRs over which payload length adaptation is critical, is wider for Rayleigh fading (up to 40 dB) compared to AWGN (less than 20 dB). It is also interesting to note from Fig. 7(b), that for Rayleigh fading, the mandatory rates of 6, 12 and 24 Mbps are used over a much wider range of SNRs compared to an AWGN environment.

C. Rate adaptation with fixed payload size

In this section we show the difference in rate adaptation and SNR thresholds for different channel conditions for a fixed payload size of 1500 bytes. In Fig. 8(a), we plot the effective throughput against SNR for all IEEE 802.11a PHY mode rates in an AWGN channel for a fixed payload size of 1500 bytes. In Fig. 8(b), we plot the effective throughput against average symbol SNR for a Rayleigh fading channel. It is interesting to observe the difference in SNR thresholds and data rates used in these two cases. In the AWGN case, all PHY modes apart from PHY mode 2 (9 Mbps), are used with the highest mode (54 Mbps) used at SNRs above 25 dB. However, in the Rayleigh fading case, neither modes 2 nor 4 corresponding to 9 Mbps and 18 Mbps, respectively, are used. Moreover, PHY mode 6 corresponding to 36 Mbps is used for an extremely narrow SNR range. This suggests that the rate 3/4 punctured convolutional codes with a lower constellation size (BPSK) are always outperformed by the larger constellation sizes (QPSK) with rate 1/2 convolutional code in Rayleigh fading for the IEEE 802.11a PHY data rates. We also plot the effective throughput against SNR for a 1500 payload size in Nakagami-m fading with $m = 4$ in Fig. 8(c). We observe

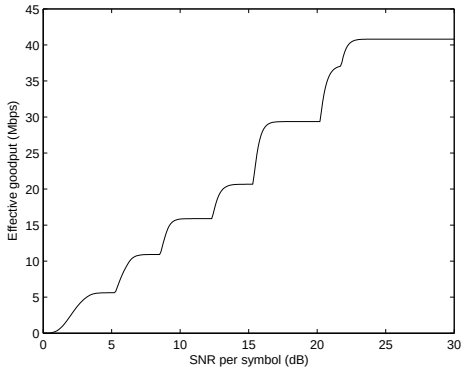

(a) Effective throughput obtained by rate and payload length adaptation in AWGN

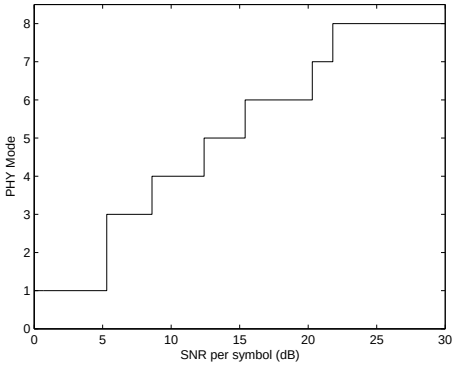

(b) Optimal rate adaptation

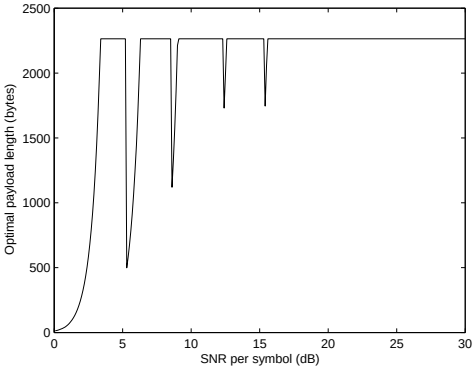

(c) Optimal payload length adaptation

Fig. 6: Optimal rate and payload length adaptation in AWGN

that as the fading decreases and approaches the AWGN case ($m \to \infty$), PHY rates 4 and 6 are used over a wider range of SNRs. The above results again indicate a tight dependence between data rate used and the appropriate channel model.

D. Link Adaptation based on Packet Error Rate

In this section, we study the impact on packet error rate of the above link adaptation schemes. The throughput and packet error rates for an AWGN channel at an SNR of 2 dB are plotted in Figs. 3 and 9, respectively. In Fig. 3 it is observed that the maximum throughput is achieved for a payload size of 280 bytes. However, from Fig. 9, this corresponds to a

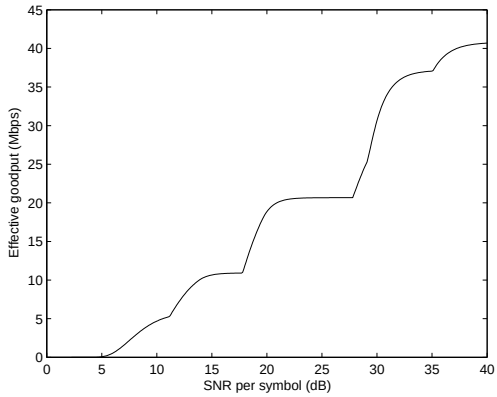

(a) Effective throughput obtained by rate and payload length adaptation in Rayleigh fading

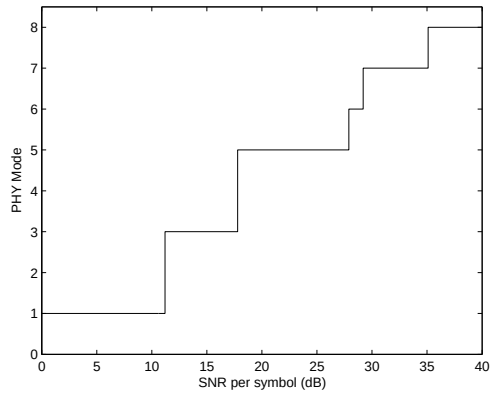

(b) Optimal rate adaptation

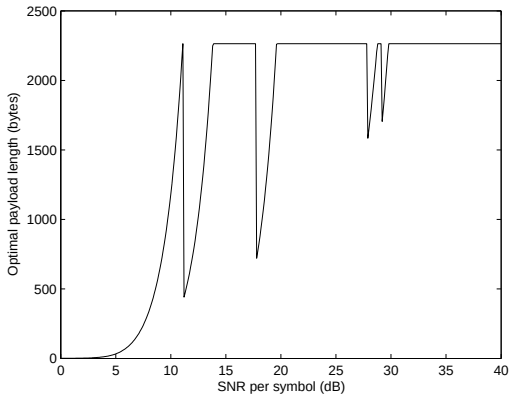

(c) Optimal payload length adaptation

Fig. 7: Optimal rate and payload length adaptation in Rayleigh fading

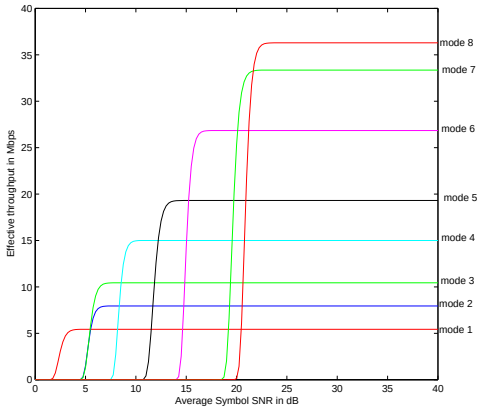

(a) Rate adaptation for 1500 byte payload length in AWGN

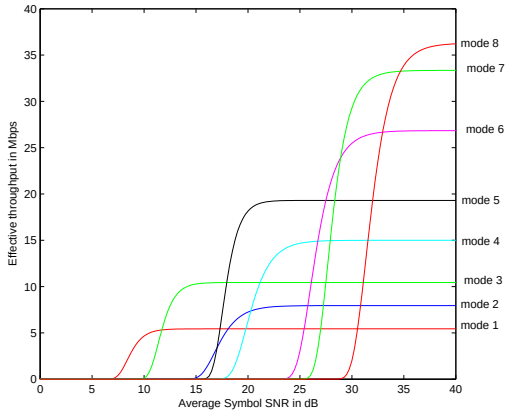

(b) Rate adaptation for 1500 byte payload length in Rayleigh fading

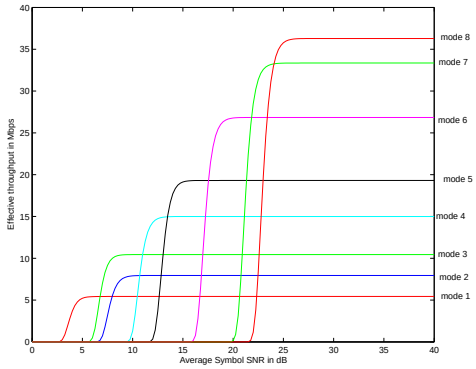

(c) Rate adaptation for 1500 byte payload length in Nakagami-m fading with m = 4

Fig. 8: Optimal rate adaptation for fixed payload lengths of 1500 bytes in different channel conditions

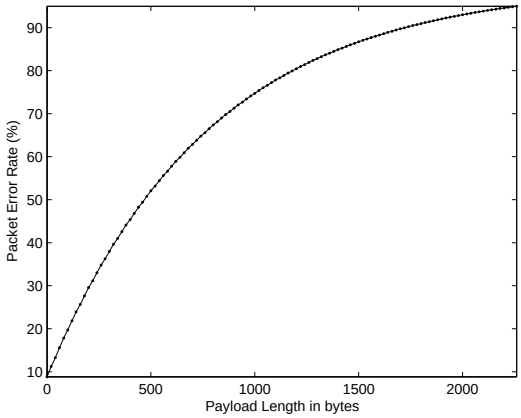

Fig. 9: Packet error rates vs SNR for various data rates with 20 bytes payload

packet error rate of 30% which can be unacceptable for certain applications. An interesting observation is that maximizing throughput does not imply minimizing packet error rate, and if packet error rate is important, link adaptation schemes should be designed to optimize effective throughput with a packet error rate constraint. This is discussed in detail in the next section.

V. Effect of payload variation on single-user throughput in fading channels

In this section, we explore the effect of payload length variation on single-user throughput by conducting simulations in multipath fading channels. We observe that the link adaptation thresholds and data rates used are significantly different from the non-fading scenario, and there is a significant degradation in performance for link adaptation schemes that fail to consider multipath fading.

In order to estimate the packet error rate under different channel conditions, we modified a readily available OFDM simulator for the IEEE 802.11a PHY [17]. The scenario we consider is of a single-user communicating with an access point or with another node. Non-fading channels as well as multipath fading channels are considered. Noise is modeled as AWGN in both scenarios. The decoding at the receiver is based on soft decision Viterbi decoding. We also assume perfect synchronization and perfect channel estimation.

The wireless channel model used for the multipath fading case is the Nafteli Chayat model [23], which is a standard indoor wireless channel model with an exponentially decaying Rayleigh faded path delay profile. The impulse response of the channel shown in Fig. 10 is composed of complex samples with uniformly distributed phase and Rayleigh distributed magnitude with an exponentially decaying average power profile. This is given by:

$$h_k = N(0, 1/2\sigma_k^2) + jN(0, 1/2\sigma_k^2) \quad (10)$$

$$\sigma_k^2 = \sigma_0^2 \exp(-k * T_s/T_{rms}) \quad (11)$$

where $N(0, 1/2\sigma_k^2)$ is a zero mean Gaussian random variable with variance $1/2\sigma_k^2$ and σ_0^2 is chosen so as to ensure $\sum_k \sigma_k^2 =$ 1 i.e., the channel coefficients are normalized so as to ensure the same average power. The rms delay spread T_{rms} used is 50 nanoseconds, which is typical for home and office environments and T_s is the sampling time

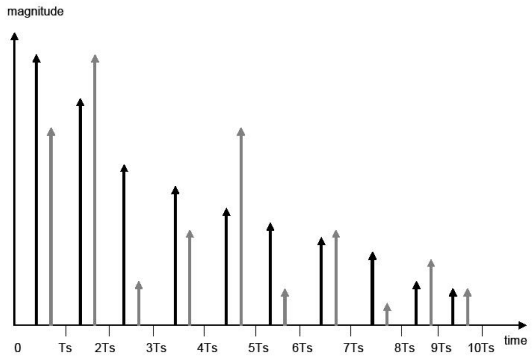

Fig. 10: Multipath channel impulse response showing average response (black) and an individual realization (grey)

The payload lengths used for our simulation purposes were 20, 200 and 2000 bytes. These values cover a wide range of voice and video applications. For the non-fading scenario, we used 1000 packets to estimate the packet error rate. The packet error rate for the fading realization was obtained by averaging over 500 fading realizations with 1000 fixed size packets per realization. This was done for the 20 and 200 bytes payload sizes. The 2000 bytes payload length was averaged over 250 fading realizations due to the higher computation time at higher payload lengths.

We define *throughput* as the number of payload bits per second received correctly as in [24]. We consider the contention-based Distributed Coordination Function (DCF) for evaluating the throughput. The MAC header and FCS consists of 28 bytes and the ACK is 14 bytes long. The RTP and UDP overhead for multimedia traffic is 12 and 8 bytes, respectively, and another 20 bytes is added for the IP header. We assume that the acknowledgments from the receiver are error-free. We also do not consider the backoff interval since we are calculating the effective throughput of a single packet transmission without considering retransmissions and collisions.

Throughput corresponding to PHY mode j and payload length L bytes is given by:

$$T(j) = \frac{L}{T_x} * R_j * (1 - PER^j(\gamma_s, L)) \quad (12)$$

where
L: payload length in bits,
T_x: Transmit time of packet including MAC and PHY headers and DCF protocol overheads,
R_j: data rate corresponding to PHY mode j,
$PER^j()$: packet error rate (PER) corresponding to PHY mode j
γ_s: Average SNR per symbol.

The packet error rate is assumed to be caused only by bit errors in the data packet in the wireless channel. The link adaptation thresholds for different payload sizes in various

channel conditions for maximizing throughput with and without a packet error rate constraint are described below.

Case a) 20 bytes payload length

The effective throughput and packet error rates vs SNR for a 20 bytes payload in a multipath fading environment are shown in Figs. 11(a) and 11(b), respectively. As mentioned earlier, 20 bytes payload corresponds to 20 ms of G.729 coded speech. The throughput obtained is significantly lower than the nominal transmitted data rate. We also tabulate the SNR thresholds for link adaptation with and without a packet error rate constraint of 5% in Tables IV and V, respectively. Table V can be obtained from Fig. 11(a) by selecting the data rate that maximizes throughput for each SNR. For instance, from 0 to 5 dB, 6 Mbps is used with a maximum throughput of 0.6 Mbps at 5 dB. At SNRs above 5 dB, 12 Mbps achieves a higher throughput (greater than 0.6 Mbps) and hence the data rate is switched to 12 Mbps. The maximum throughput at 12 Mbps data rate using 20 bytes payload is around 1 Mbps and this is achieved at 12 dB. At SNRs above 12 dB, the data rate is switched to a higher PHY mode (PHY mode 4 corresponding to 24 Mbps). By repeating this procedure for all the data rates and SNR values, the SNR thresholds for link adaptation for throughput optimization for 20 bytes payload length can be obtained from Fig. 11(a).

TABLE IV: Link adaptation thresholds using 20 bytes payload with maximum packet error rate constraint of 5% in a frequency selective multipath fading environment

Data Rate(Mbps)	6	12	18	24	36	48
SNR range(dB)	7-10	10-14	14-15	15-20	20-23	> 23

TABLE V: Link adaptation thresholds using 20 bytes payload without packet error rate constraint in a frequency selective multipath fading environment

Data Rate (Mbps)	6	12	24	36	48
SNR range (dB)	0-5	5-12	12-20	20-22	> 22

The above link adaptation scheme does not account for packet losses. In multimedia applications, packet losses have a significant impact on perceived quality and high packet losses (more than 5 to 10% packet error rate) cannot be easily concealed. Furthermore, retransmissions might result in higher latency and cause significant congestion in the wireless link so we do not consider retransmissions in this work. Observe that although the 6 Mbps data rate optimizes throughput for SNRs from 0 to 5 dB, Fig. 11(b) shows that the packet loss rate varies from 10 to 80%, which would be far too high for multimedia applications. Hence, for multimedia applications, we need to impose a packet error rate constraint when maximizing throughput. Therefore, in the following we consider a link adaptation scheme that maximizes the throughput given a maximum packet error rate constraint of 5%. The link adaptation thresholds for this scheme with a packet error rate constraint are tabulated in Table IV with the

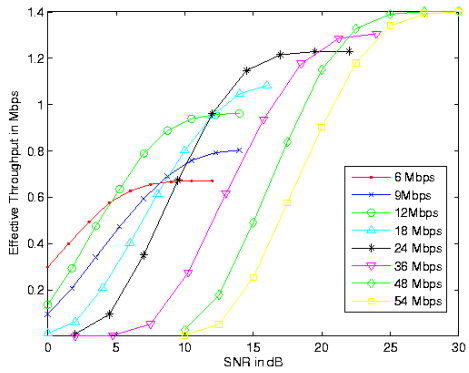

(a) Effective Throughput vs SNR for various data rates with 20 bytes payload

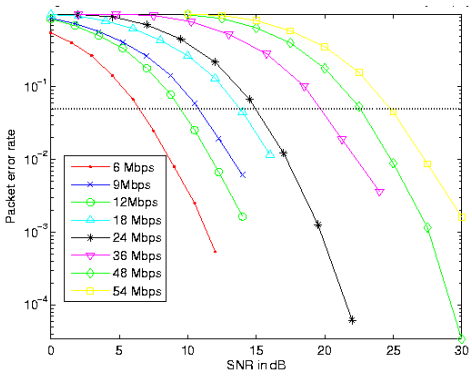

(b) Packet error rates vs SNR for various data rates with 20 bytes payload

Fig. 11: Effective Throughput and packet error rates vs SNR for 20 bytes payload in frequency selective multipath fading

SNR thresholds obtained from Fig. 11(b) in a similar manner as described above. As can be seen from the tables, there is a substantial shift in the SNR thresholds for optimal adaptation with and without a packet eror rate constraint. For instance, PHY mode 1 (6 Mbps) is used from 0 to 5 dB without a packet error rate constraint. However, it can only be used at SNRs of 7-10 dB when a packet error rate constraint of 5% is introduced.

It is interesting to observe that the 9 Mbps data rate is not used over the various SNR ranges. This is also observed at the higher payload cases as well. This has been widely described in the literature [2] and has been attributed to the poor frequency selectivity characteristics of the punctured convolutional codes. Note that though mode 4 (18 Mbps PHY rate) is not used when the packet error rate constraint is neglected, it does play a role from 14-15 dB when a PER of 5% is considered. Furthermore, mode 8 corresponding to 54 Mbps is not used in either case though the PER using this data rate is less than 5 % at SNRs greater than 24.75 dB. The data rate is not switched to 54 Mbps since a higher effective throughput cannot be obtained using 54 Mbps for a 20 bytes payload size. At SNRs above 28 dB, the effective throughput obtained using both the data rates (48 Mbps and 54 Mbps) are equal to 1.4 Mbps (with packet error rate less than 5 % for

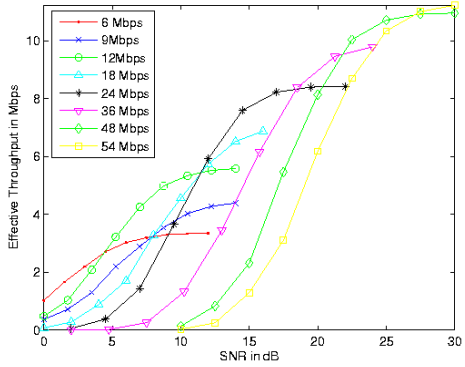

(a) Effective Throughput vs SNR for various data rates with 200 bytes payload

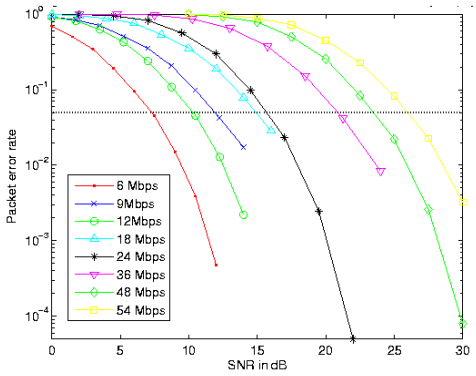

(b) Packet error rates vs SNR for various data rates with 200 bytes payload

Fig. 12: Effective Throughput and packet error rates vs SNR for 200 bytes payload in frequency selective multipath fading

both data rates) and hence, an unnecessary data rate switching is avoided for both link adaptation schemes.

Case b) 200 bytes payload length

The effective throughput and packet error rates vs SNR for 200 bytes payload in a multipath fading environment are shown in Figs. 12(a) and 12(b), respectively. The SNR thresholds for optimal rate adaptation with and without a packet error rate constraint are tabulated in Tables VI and VII, respectively. As expected (similar to the 20 bytes payload length case), much higher SNRs are required when a packet error rate constraint is imposed on the link adaptation scheme. By comparing Tables IV and VI as well as Tables V and VII, it is observed that the SNR thresholds obtained by both link adaptation schemes are dependent on the payload size. For instance, mode 8 (54 Mbps) which was not used for 20 bytes payload size is used for 200 bytes payload size at SNRs above 27 dB.

Case c) 2000 bytes payload length

The effective throughput and packet error rates vs SNR for 2000 bytes payload in multipath fading environment are shown in Figs. 13(a) and 13(b), respectively. As in the non-fading scenario, a significant gain in throughput for the larger payload

TABLE VI: Link adaptation thresholds using 200 bytes payload with maximum packet error rate constraint of 5% in a frequency selective multipath fading environment

Data Rate(Mbps)	6	12	18	24	36	48	54
SNR range(dB)	7-10	10-15	15-16	16-21	21-24	24-27	>27

TABLE VII: Link adaptation thresholds using 200 bytes payload without packet error rate constraint in a frequency selective multipath fading environment

Data Rate(Mbps)	6	12	24	36	48	54
SNR range(dB)	0-5	5-12	12-19	19-22	22-27	>27

length is observed. A larger payload size of 2000 bytes can be used for video transmission at good channel conditions. The SNR thresholds for optimal rate adaptation with and without a packet error rate constraint are tabulated in Tables VIII and IX, respectively. By comparing the SNR thresholds for the different payload sizes, we again observe the importance of payload size and packet error rates for link adaptation schemes. For instance, as observed from Table IV, the operating SNR thresholds with a 5% packet error rate constraint varies from 7 to 23 dB for a 20 bytes payload size (with 54 Mbps not being used) whereas for 2000 bytes payload length as seen from Table VIII, the SNR thresholds vary from 9 to 27 dB with 54 Mbps used at SNRs above 27 dB.

TABLE VIII: Link adaptation thresholds using 2000 bytes payload with maximum packet error rate constraint of 5% in a frequency selective multipath fading environment

Data Rate(Mbps)	6	12	18	24	36	48	54
SNR range(dB)	9-12	12-16	16-17	17-22	22-25	25-27	>27

TABLE IX: Link adaptation thresholds using 2000 bytes payload without packet error rate constraint in a frequency selective multipath fading environment

Data Rate(Mbps)	6	12	24	36	48	54
SNR range(dB)	0-4	4-11	11-17	17-20	20-25	>25

In order to contrast the impact of multipath fading channels with AWGN only channels (or fading channels where the average SNR is estimated based on path loss and shadowing only, without taking into account the effects of multipath fading) the throughput and packet error rates for a 2000 byte payload length are shown in Figs. 14(a) and 14(b), respectively. The link adaptation thresholds with and without packet error rate constraints are in Tables X and XI, respectively. By comparing Tables VIII and X, we observe that in an AWGN only channel PHY mode 1 (6 Mbps) can be used from 1 to 4 dB whereas in a multipath fading channel, it is used from 9 to 12 dB. Similarly, PHY mode 8 (54 Mbps) is used at SNRs above 19 dB in an AWGN channel whereas in a multipath fading channel, it can be used only at SNRs above 27 dB. Hence, the performance of link adaptation schemes are very much

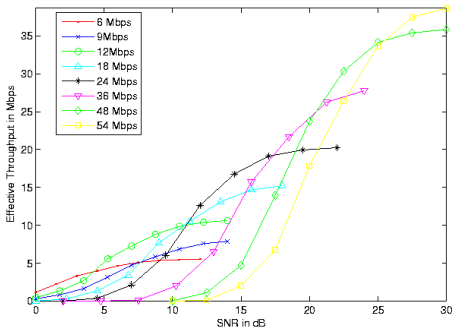

(a) Effective Throughput vs SNR for various data rates with 2000 bytes payload

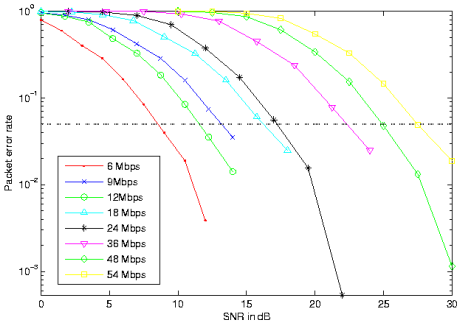

(b) Packet error rates vs SNR for various data rates with 2000 bytes payload

Fig. 13: Effective Throughput and packet error rates vs SNR for 2000 bytes payload in frequency selective multipath fading

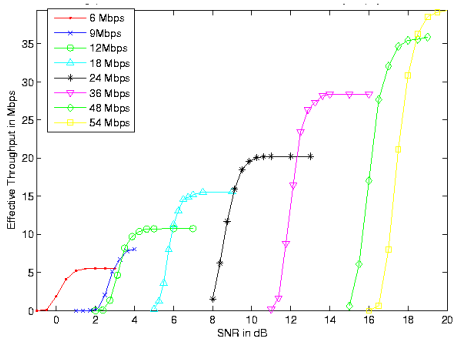

(a) Effective Throughput vs SNR for various data rates with 2000 bytes payload in non-fading AWGN channels

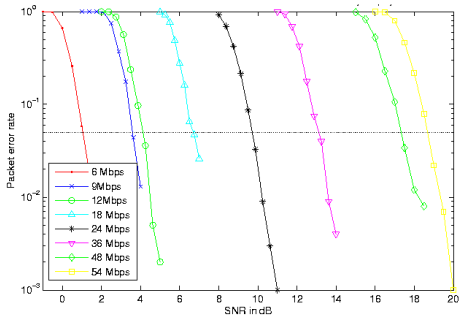

(b) Packet error rates vs SNR for various data rates with 2000 bytes payload in non-fading AWGN channels

Fig. 14: Effective Throughput and packet error rates vs SNR for 2000 bytes payload in non-fading AWGN channels

dependent on the channel models assumed. Link adaptation schemes where the SNR is estimated purely on path loss and shadowing have very different operating SNR regions when the impact of multipath fading is considered.

TABLE X: Link adaptation thresholds using 2000 bytes payload with maximum packet error rate constraint of 5% in a non-fading environment

Data Rate(Mbps)	6	12	18	24	36	48	54
SNR range (dB)	1-4	4-7	7-10	10-13	13-17	17-19	>19

TABLE XI: Link adaptation thresholds using 2000 bytes payload without packet error rate constraint in a non-fading environment

Data Rate (Mbps)	6	12	18	24	36	48	54
SNR range (dB)	1-3	3-6	6-9	9-12	12-16	16-18	>18

VI. Conclusions

We have presented a theoretical framework for achieving higher throughputs by careful adaptation of payload length and data rates with varying channel conditions under the assumption of AWGN and slowly varying flat fading Nakagami-m channels. The packet headers and protocol overheads reduce the effective throughput drastically, motivating the need for link adaptation with varying channel conditions. We present plots for payload length and rate selection for maximizing the single user throughput over a wireless link based on the average received SNR per symbol or an equivalent packet error rate. We also show the strong dependence of payload and rate adaptation on the wireless channel condition. The link adaptation algorithm does not involve any changes in the current MAC as the data rate and payload length can be adapted based on the received SNR. We also observe that the link adaptation thresholds are dependent on the fading environment. Any link adaptation scheme that dynamically adjusts the thresholds based on the existing fading realization will outperform schemes that use precomputed thresholds. Moreover, link adaptation schemes that consider only path loss and shadowing will perform significantly worse in the presence of multipath fading. We also observed that link adaptation thresholds are quite sensitive to received SNR estimates - hence accurate SNR estimation and low delay feedback of SNR estimates to the transmitter needs to be considered. We are also investigating cross-layer design schemes with adaptive payload selection and rate adaptation for video transmission over IEEE 802.11a wireless networks.

Acknowledgment

The authors would like to thank Jing Hu for contributing Table I and for many valuable discussions on applications to

video transmission.

REFERENCES

[1] "IEEE 802.11a, Part11: Wireless LAN Medium Access Control (MAC) and Physical Layer (PHY) Specifications: High-Speed Physical Layer in the 5GHz Band," *supplement to IEEE 802.11 Standard*, 1999.

[2] D. Qiao, S. Choi, and K. G. Shin, "Goodput Analysis and Link Adaptation for IEEE 802.11a Wireless LANs," *IEEE Transactions on Mobile Computing*, vol. 1, no. 4, 2002.

[3] S. Catreux, V. Erceg, D. Gesbert, and R. W. Heath, Jr., "Adaptive Modulation and MIMO Coding for Broadband Wireless Data Networks," *IEEE Communications Magazine*, pp. 108–115, June 2002.

[4] J. Hu, S. Choudhury, and J. Gibson, "PSNRr,f: Assessment of Delivered AVC/H.264 Video Quality over 802.11a WLANs with Multipath Fading," *Multicomm 2006*, June 2006.

[5] D. P. Hole and F. A. Tobagi, "Capacity of an IEEE 802.11b wireless LAN supporting VoIP," *Proceedings of IEEE ICC 2004*, pp. 196–201, June 2004.

[6] P. Lettieri and M. B. Srivastava, "Adaptive Frame Length Control for Improving Wireless Link Throughput, Range and Energy Efficiency," in *INFOCOM (2)*, pp. 564–571, 1998.

[7] J. P. Pavon and S. Choi, "Link Adaptation Strategy for IEEE 802.11 WLAN via Recieved Signal Strength Measurement," in *Proceedings of IEEE ICC 2003*, pp. 1108–1113, May 2003.

[8] A. Kammerman and L. Monteban, "WaveLAN-II: A High-Performance Wireless LAN for the Unlicensed Band," *Bell Labs Technical Journal*, pp. 118–133, 1997.

[9] G. Holland, N. Vaidya, and P. Bahl, "A Rate-Adaptive MAC Protocol for Multi-Hop Wireless Networks," *Proceedings of ACM Mobicom'01*, pp. 236–251, 2001.

[10] Z. Lin, G. Malmgren, and J. Torsner, "System Performance Analysis of Link Adaptation in HiperLAN Type 2," *Proceedings of IEEE VTC 2000 (Fall)*, pp. 1719–1725, May 2000.

[11] J. Habetha and D. de No, "New Adaptive Modulation and Power Control Algorithms for HIPERLAN/2 Multihop Ad Hoc Networks," *Proceedings of European Wireless*, Sept. 2000.

[12] S. Armour, A. Doufexi, A. Nix, and D. Bull, "A study of the impact of frequency selectivity on link adaptive wireless LAN systems," in *Proceedings of IEEE VTC 2002 (Fall)*, pp. 738–742, Sept. 2002.

[13] A. Doufexi, S. Armour, M. Butler, A. Nix, D. Bull, and J. McGeehan, "A comparison of the HIPERLAN/2 and IEEE 802.11a wireless lan standards," *IEEE Communications Magazine*, vol. 40, pp. 172–180, May 2002.

[14] Y. Xiao and J. Rosdahl, "Throughput and delay limits of IEEE 802.11," *IEEE Communications Letters*, vol. 6, pp. 355–357, Aug. 2002.

[15] "IEEE 802.11 Wireless LAN Medium Access Control (MAC) and Physical Layer (PHY) Specification," *Standard, IEEE*, Aug. 1999.

[16] R. van Nee and R. Prasad, *OFDM for Wireless Multimedia Communications* . Artech House, Jan 2000.

[17] J. Heiskala and J. Terry, *OFDM Wireless LANs: A Theoretical and Practical Guide* . Sams Publishing, December 2001.

[18] M. B. Pursley and D. J. Taipale, "Error Probabilities for Spread-Spectrum Packet Radio with Convolutional Codes and Viterbi Decoding," in *IEEE Transactions on Communications*, vol. COM-35, pp. 1–12, Jan. 1987.

[19] C. Lee and L. H. C. Lee, *Convolutional Coding: Fundamentals and Applications*. Artech House Publishers, 1997.

[20] J. G. Proakis, *Digital Communications*. McGraw-Hill, 4th ed., 2000.

[21] M. K. Simon and M.-S. Alouini, *Digital Communication over Fading Channels*. Wiley-IEEE Press, 2nd ed., November 2004.

[22] S. Choudhury, I. Sheriff, J. Gibson, and E. Belding-Royer, "Effect of Payload Length Variation and Retransmissions on Multimedia in 802.11a WLANs," *International Wireless Communications and Mobile Computing Conference*, July 2006.

[23] N. Chayat, "Tentative Criteria for Comparison of Modulation Methods," *IEEE P802.11-97/96*, Sept. 1997.

[24] M. B. Pursley and J. M. Shea, "Adaptive nonuniform phase-shift-key modulation for multimedia traffic in wireless networks," in *IEEE Journal on Selected Areas in Communications*, vol. 18, pp. 1394–1407, Aug. 2000.

Sayantan Choudhury received his B.E. in Electrical Engineering from Jadavpur University, Calcutta in 2000. He received his M.S. in Electrical Engineering at the University of Texas at Austin in 2003 specializing in communications, networks and systems. Since Fall of 2003, he has been pursuing his Ph.D. in Electrical Engineering at the University of California, Santa Barbara specializing in communications, controls and signal processing . He advanced to PhD candidacy in December, 2004. Sayantan's research focuses on cross layer design and link adaptation for multimedia communications over wireless local area networks. He is affiliated with the Vivonets Lab, Signal Compression Laboratory and Multimedia Research Group.

Jerry D. Gibson is Professor of Electrical and Computer Engineering and Professor in the Media Arts & Technology Graduate Program at the University of California, Santa Barbara. He is co-author of the books *Digital Compression for Multimedia* (Morgan-Kaufmann, 1998) and *Introduction to Nonparametric Detection with Applications* (Academic Press, 1975 and IEEE Press, 1995) and author of the textbook, *Principles of Digital and Analog Communications* (Prentice-Hall, second ed., 1993). He is Editor-in-Chief of *The Mobile Communications Handbook* (CRC Press, 2nd ed., 1999), Editor-in-Chief of *The Communications Handbook* (CRC Press, 2nd ed., 2002), and Editor of the book, *Multimedia Communications: Directions and Innovations* (Academic Press, 2000).

Dr. Gibson was Associate Editor for Speech Processing for the *IEEE Transactions on Communications* from 1981 to 1985 and Associate Editor for Communications for the *IEEE Transactions on Information Theory* from 1988-1991. He was President of the IEEE Information Theory Society in 1996, and a member of the Speech Technical Committee of the IEEE Signal Processing Society from 1992-1994. Dr. Gibson served as Technical Program Chair of the 1999 IEEE Wireless Communications and Networking Conference, Technical Program Chair of the 1997 Asilomar Conference on Signals, Systems, and Computers, and General Co-Chair of the 1993 IEEE International Symposium on Information Theory. Currently, he serves on the Steering Committee for the Wireless Communications and Networking Conference, and he is an elected Member-at-Large on the Communications Society Board of Governors for 2005-2007. He serves on the Editorial Boards of the *IEEE Transactions on Information Forensics and Security* and the Hindawi Open Access journal *Advances in Multimedia*.

In 1990, Dr. Gibson received The Fredrick Emmons Terman Award from the American Society for Engineering Education, and in 1992, was elected Fellow of the IEEE for contributions to the theory and practice of adaptive prediction and speech waveform coding. He was co-recipient of the 1993 IEEE Signal Processing Society Senior Paper Award for the Speech Processing area.

His research interests include data, speech, image, and video compression, multimedia over networks, wireless communications, information theory, and digital signal processing.